Probing the positron moderation process using high-intensity, highly polarized slow-positron beams

J. Van House
Physics Department, University of Michigan, Ann Arbor, Michigan 48109

P. W. Zitzewitz
Department of Natural Sciences, University of Michigan—Dearborn, Dearborn, Michigan 48128
(Received 11 April 1983)

We have generated a highly polarized ($P=0.48\pm0.02$) intense (5×10^5/sec) beam of "slow" ($\Delta E\sim2$ ev) positrons (e^+) and shown that it is possible to achieve polarization as high as $P=0.69\pm0.04$ with reduced intensity. The measured polarization of the slow e^+ emitted by five different positron moderators showed no dependence on the moderator atomic number (Z). This allows us to conclude that only source positrons with final kinetic energy below 17 keV contribute to the slow-e^+ beam, in disagreement with recent yield functions derived from low-energy measurements. Measurements of polarization and yield with absorbers of different Z between the source and moderator show the effects of the energy and angular distributions of the source positrons on P. The depolarization of fast positrons transmitted through high-Z absorbers has been measured. Applications of polarized slow-e^+ beams are discussed.

I. INTRODUCTION

The discovery[1] that the slow (~1 eV) positrons (e^+) emitted from MgO moderators are spin polarized has recently been used to test one hypothesis of the origin of optical activity in biological molecules[2] and to investigate the spin polarization of electrons at the surface of Ni(110).[3] Additional applications include polarized low-energy positron diffraction (PLEPD) as a complement to low-energy positron diffraction[4] (LEPD) and studies of the slow-positron-emission process itself. This paper reports a study of the slow-positron-emission process, which has enabled us to produce high-intensity slow-positron beams with polarizations as large as 0.69 ± 0.04.

The currently accepted model of the slow-e^+-emission process[5] asserts that fast positrons from a radioactive source (see Fig. 1) injected into a moderator lose energy through a variety of collision processes until they reach energies near 0.1 eV. In the subsequent thermal diffusion process a few reach the surface where they can be ejected with energies (of order 1 eV) determined by the negative work function of the moderator. The polarization of these slow e^+ is determined by properties of the radioactive nuclei and source holder, the source-moderator geometry (including the effects of any absorbers between the source and moderator), and depolarization in the moderation and ejection processes.

According to the V-A theory of the weak interaction, positrons emitted from a nucleus possess an helicity or longitudinal polarization $h\equiv\langle\vec{\sigma}_i\cdot\hat{p}_i\rangle=\langle v_i/c\rangle$, where for each individual e^+, $\vec{\sigma}_i$ is the Pauli spin matrix, $\hat{p}_i$ the e^+ unit momentum, v_i the e^+ speed, and c the speed of light. This relationship determines the distribution of the source-positron spins as a function of energy. The angle between the incident e^+ velocity and the normal to the source determines the angular spin distribution. The polarization of the slow-e^+ ensemble will depend on this spin distribution averaged over all angles admitted to the moderator and all initial energies effective in forming slow e^+. Backscattering from the source will reduce the average magnitude of the source polarization by introducing e^+ of reversed spin into the source spin distribution. Placement of absorbers between the source and moderator (see Fig. 1) will modify the source spin distribution by elimination of low-energy e^+ with their low helicity from the source spectrum and by preferential attenuation of source e^+ emitted at large angles relative to the normal.

The depolarization which results from the scattering that occurs during the process of thermalization depends

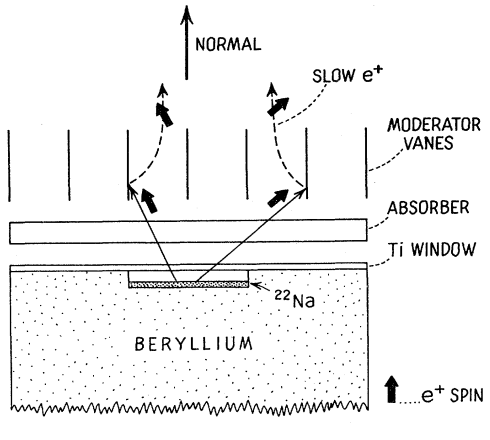

FIG. 1. Source-absorber-moderator details. Representative paths for two source positrons are shown, with the resulting spin of the slow positrons. The normal is also defined.

on the initial kinetic energy of the source e^+ as well as the atomic number (Z) of the medium in which the positron slows down.[6] Depolarization may occur during the diffusion process through spin-dependent interactions with the electrons or ion cores of the moderator (similar to muon spin relaxation). It may also occur in the emission process if, as has been suggested,[7] orthopositronium (o-Ps) is formed within the moderator and then field ionized as it is ejected through the surface of the moderator. The results of this paper measure or set limits on all these processes.

II. SLOW-POSITRON POLARIMETRY

A. Slow-positron beam

For these studies long-lived (2.6 y half-life) ^{22}Na sources (prepared by New England Nuclear Corp.) were used. To reduce backscattering, with its resultant reduction of polarization, the source support was constructed of low-Z beryllium (Be) metal. In one source 22 mCi were drop deposited in a 60° half-angle cone drilled in the Be resulting in emission into π steradians. In the second, 47 mCi were drop deposited on an insulin wetting agent in a 0.25-mm deep, 3.5-mm diameter cylindrical depression milled in the Be, resulting in emission into 2π sr. Both sources were sealed with 2.2-mg/cm^2 thick Ti windows. The insulin results in formation of very small crystals of $NaC_2H_3O_2$ uniformly deposited with a $\sim$1 mg/cm^2 thickness.[8] This produces only 4% self-absorption of positrons in comparison with the 16% self-absorption suffered by positrons in the 6±2 mg/cm^2 deposit in the cone-shaped depression.

A variety of moderator materials have been used in these studies. All use a "Venetian-blind" geometry with the moderator surface parallel to the beam direction, so positrons are incident on the vanes at almost glancing angles (see Fig. 1). In earlier work the moderator of choice in non-UHV slow-positron beams was MgO smoked on a metallic substrate (Venetian blind, thin film, or grids).[9] Studies of the effect of substrate geometry on yield showed a fourfold increase could be obtained over the geometry of Ref. 9 by using a thin slice of "Hexcell" (Hexcell Corp.), a honeycomblike structure of 0.02-mm thick aluminum foil. Cell widths of 1.5, 3, and 6 mm were used; in each case the optimum cell length was equal to the cell width.

The large energy width (ΔE) of the slow e^+ emitted from MgO (measured to be $\Delta E = 5$ eV at the moderator) causes difficulty in forming a tightly focused "bright" beam,[10] prompting a search for moderators with smaller ΔE. To this end, well-annealed samples of Pt, W, Mo, Ta, and Cu were used. The details of their preparation may be found in the Appendix.

The slow e^+ emitted from a moderator are electrostatically collected and focused into a beam which enters the Wien filter where the particle spins ($\vec{s}_i$) are rotated through a selected rotation angle. The undeflected beam is then bent 90° through a cylindrical mirror energy analyzer (CMA) and electrostatically transported to the slow-positron polarimeter.

B. Positron polarimeter

The slow-positron polarimeter[1] is shown in Fig. 2. The beam enters along the axis of the 6.5 kG magnetic field through a hole in one of the pole pieces and strikes the surface of a chevron electron-multipler array (CEMA) (Galileo Electro-Optics 3025) at an energy of 500 eV. The 500-eV e^+ generate secondary electrons which are collected by the CEMA to form a start pulse for a time-to-amplitude converter (TAC). About 10% of the incident positrons capture an electron and form orthopositronium (o-Ps) which leaves the CEMA surface and enters the MgO-coated confinement cavity. The subsequent annihilation γ rays (stop signal) are detected in Nuclear Enterprise Inc. (NEI) Pilot B plastic scintillators coupled to four Amperex XP 2020 photomultipliers. The lifetime of each positron event is directly measured and recorded using a TAC-multichannel analyzer system.[11]

The operation of the polarimeter[12,13] is based on the fact that in a magnetic field the $m=0$ singlet and $m=0$ triplet positronium substates are mixed to form two field-perturbed states. Not only does magnetic mixing increase the decay rate λ' of the perturbed triplet state, but it also renders the fraction of positronium formed in this state dependent on the quantity $\vec{S}\cdot\vec{B}$, where $\vec{S}\equiv\langle\vec{s}_i\rangle$ and $\vec{B}$ is the magnetic field. For times sufficiently beyond the prompt peak of free annihilation and singlet decays the time spectrum of triplet positronium decay, shown graphically in Fig. 3, is

$$\frac{dN(t)}{dt}=\frac{N}{4}[2\lambda e^{-\lambda t}+(1-\eta P\cos\theta)\lambda' e^{-\lambda' t}]\ . \qquad (1)$$

Here $P\equiv 2|\vec{S}|$, N is the total number of positronium atoms formed, λ is the magnetically unperturbed ($m=\pm 1$) decay rate including all quenching mechanisms ($\lambda^{-1}=140$ nsec), and θ is the angle between $\vec{S}$ and $\vec{B}$. The parameter η is given by $\eta=\chi/(1+\chi^2)^{1/2}$, where $\chi=0.0276B$ for B in kG and $\lambda'=(\lambda+y^2\lambda_s)/(1+y^2)$, where $\lambda_s^{-1}=0.125$ nsec and $y=\chi/[1+(1+\chi^2)^{1/2}]$. At 6.5 kG, $(\lambda')^{-1}=15$ nsec

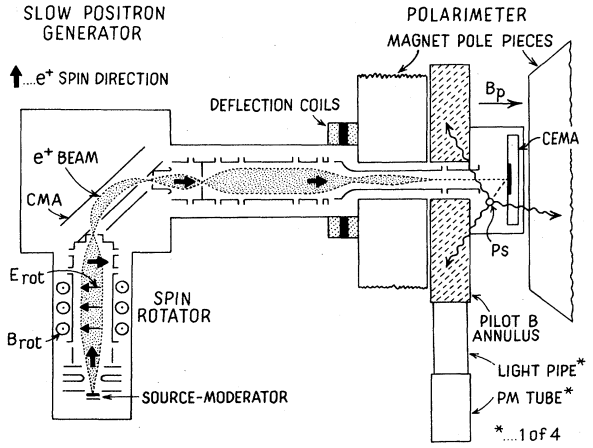

FIG. 2. Slow-positron beam generator and polarimeter. The crossed fields $B_{\rm rot}$ and $E_{\rm rot}$ form the Wien filter spin rotator.

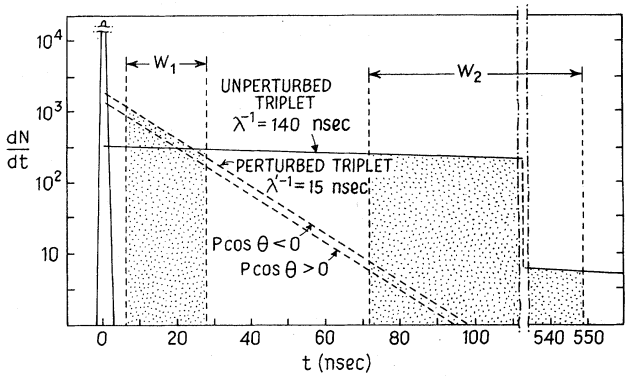

FIG. 3. Spectrum of Ps decay in a magnetic field showing the prompt peak and components due to perturbed triplet and unperturbed triplet decay. The two time windows, W_1 and W_2, are also shown.

and $\eta=0.176$. Thus, decays from the perturbed state can be distinguished from decays from the magnetically unperturbed states by their shorter lifetime. By measuring changes in the intensity of the perturbed triplet component relative to the intensity of the unperturbed triplet component when the positron spin direction or the magnetic field direction is varied (see Fig. 3), the quantity ηP can be determined.

The relative intensity of the perturbed triplet component is measured by accumulating counts in two separate time windows in the background corrected lifetime spectrum. The perturbed window W_1, from $t_1=6$ nsec to $t_2=28$ nsec, is composed primarily of decays from the perturbed triplet state. The normalization window W_2, from $t_3=72$ nsec to $t_4=548$ nsec, is composed (99%) of unperturbed decays. The ratio (R) of counts in W_1 to counts in W_2 is proportional to the relative perturbed triplet intensity. By forming this ratio for $\vec{S}\cdot\vec{B}>0$ (R_+) and then, upon reversal of the direction of $\vec{B}$ or $\vec{S}$, for $\vec{S}\cdot\vec{B}<0$ (R_-), the polarization for $\cos\theta=\pm1$ can be determined from the relation

$$P=\frac{-1}{\eta f}\frac{(R_+-R_-)}{(R_++R_-)}=\frac{-1}{2\eta f}\frac{\Delta R}{\bar{R}}\ . \tag{2}$$

$\bar{R}$ is the ratio that would be obtained for an unpolarized beam and f is the fraction of events in W_1 due to decays from the $m=0$ state. This fraction is determined from a separate run at $B=0$ [$f=1-R(B=0)/\bar{R}$].

Three systematic effects which reduce the measured value of the beam polarization have been studied. The first is an overestimate of the fraction f of counts in W_1 due to perturbed triplet-Ps decays. The second is the depolarization of the positrons in the polarimeter in the magnetic field gradient at the entrance to the polarimeter. The third is the rotation of the positron spins away from the direction of $\vec{B}$ due to stray magnetic fields seen by the beam before entering the polarimeter.

The determination of the beam polarization P from ratios of counts in time windows [Eq. (2)] requires that only unperturbed triplet-Ps or perturbed triplet-Ps events contribute to the two windows. Since the publication of Ref. 1 a source of unperturbed events in W_1 has been found which exists only when the magnetic field is on, resulting in an incorrect calculation of f. Positrons which strike the CEMA, giving rise to a start signal, can annihilate promptly, form Ps, or be backscattered from the CEMA. When $B=0$ essentially all of these positrons reach a metallic surface within 1 nsec, annihilate, and contribute to the prompt peak. However, when the magnetic field is on, the motion of the positrons is constrained to the beam axis. While some positrons leave the polarimeter and escape detection, others can be returned by the lens system to the CEMA up to 30 nsec after their first arrival, with the time determined by their axial energy. These decay events contribute to the perturbed window. Because more than 97% of these returning positrons will not form perturbed Ps, they will give rise to an increased value of $\bar{R}$ without a corresponding increase in $R(B=0)$. Thus the calculated value of f will be too large and P too small.

To return all backscattered positrons to the CEMA before the start of W_1, an electric field is established by setting the voltage of the last lens V_L, below the 500 V potential on the surface of the CEMA. As this field is increased by lowering V_L, the time required for the backscattered positrons to be returned to the CEMA decreases, allowing fewer to produce prompt events in W_1, and thus lowering the value of $\bar{R}$. When $V_L=0$, all are returned within 3 nsec, well before the start of W_1. This reduction in the number of events in W_1 is partially canceled by the increased number of backscattered positrons returned to the CEMA by the higher fields.

The determination of the correct values to use in Eq. (2) is complicated by the reduced intensity of the beam transmitted to the CEMA as V_L is lowered. At $V_L=0$ none reach the CEMA, requiring an extrapolation of P to $V_L=0$. Figure 4 shows two methods of correcting for

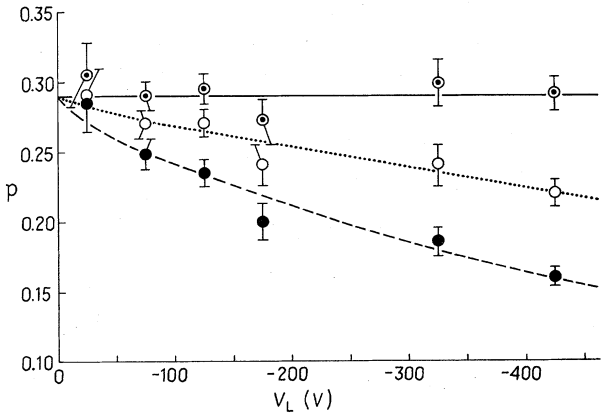

FIG. 4. Effect on polarization of the last lens voltage. The solid cricles show the polarization calculated from Eq. (2). The open circles include the correction for the effect of backscattered positrons. The circled dots are corrected for both backscattered positrons and depolarization due to windup in the magnetic field gradient. The least-squares fit of the solid line shows that effects of V_L on P are reduced to $(1\pm40)\times10^{-6}$/V.

these backscattered positrons in the calculation of the true beam polarization. The solid points and the dashed curve were calculated using the uncorrected values of $\bar{R}$ at each V_L. The extrapolation of P to $V_L=0$ determines the true beam polarization and the true value of f and $\bar{R}$, corrected for backscattered positrons. These values were then used to calculate the open circles and the dotted line. The variation of these corrected values of P with V_L shows that a second systematic effect, also dependent on V_L, is present.

This second systematic effect is caused by the gradient in the magnetic field at the entrance to the polarimeter. Any positron whose position and momentum are not precisely along the axis will have some kinetic energy transferred from axial to cyclotron motion. This transfer was measured by using the last lens as a retarding field analyzer, resulting in the differential energy spectrum of the axial motion shown in Fig. 5.

The positrons which suffer this transfer of energy are depolarized due to the conservation of $\vec{S}\cdot\vec{p}$ for small numbers of cyclotron revolutions. (Here $\vec{p}=\langle\vec{p}_i\rangle$ is the beam momentum.) The resulting "winding up" of the beam reduces the projection of $\vec{S}$ along the magnetic field axis and thus the measured polarization. In the operation of the polarimeter, the field provided by V_L removes those positrons which have lost axial kinetic energy and thus have been depolarized. When $V_L=0$, only those positrons with totally axial kinetic energy will be admitted to the polarimeter. The correction to the measured polarization for $V_L\neq 0$ can be calculated by averaging the momentum transferred to cyclotron motion over the momentum spectrum $[N(p_i)]$ to obtain

$$\frac{P_f}{P_I}\equiv\langle\cos\theta\rangle=\left[\sum_{p_i=p_1}^{p_2}N(p_i)p_i\right]\left[\sum_{p_i=p_1}^{p_2}N(p_i)\right]^{-1}. \quad (3)$$

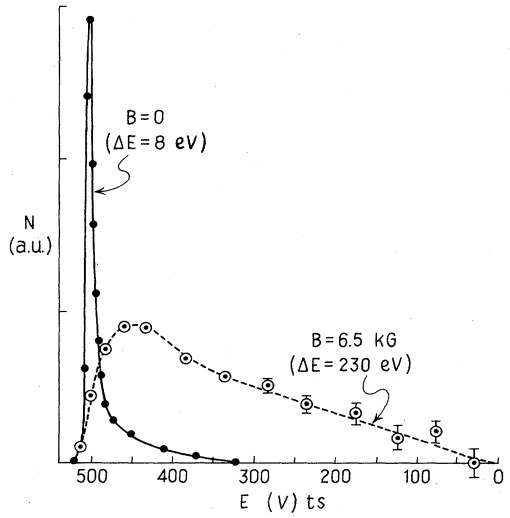

FIG. 5. Differential energy-loss spectra of the e^+ emitted by the MgO moderator at $B=0$ and 6.5 kG, measured by using the last lens of the polarimeter as a retarding field energy analyzer. The measured energy spread at $B=0$ is larger at the polarimeter than at the moderator because of the poorer resolution of this analyzer. The number of counts N is in arbitrary units.

Here p_2 is the positron momentum before transmission through the gradient, p_1 is the lowest positron momentum energetically allowed to reach the CEMA, as determined by the last lens voltage, $N(p_i)$ is obtained from the *energy* spectrum, P_I is the positron polarization before transmission through the gradient, and P_f is the polarization after passing through the gradient. Changing the retarding field by varying the last lens voltage changes the lower limit of the summation of Eq. (3) resulting in different calculated values of depolarization ranging from $P_f/P_I=0.75$ for $V_L=-400$ to $P_f/P_I=0.97$ for $V_L=-20$. The dotted curve in Fig. 2 shows that the calculated values of P at different values of V_L, based on the value of P measured at $V_L=0$, are in excellent agreement with the measured polarizations.

Stray magnetic fringing fields in the beam path can rotate the positron-beam spin direction ($\vec{S}$). Rotation within the plane of the Wien filter spin rotator can be detected by the shift in phase of the spin-rotator (SR) curve, that is, the displacement of the extrema in R from the calculated rotation angles 0° and 180°. While the rotation in the plane of the Wein filter can be measured, rotation out of the plane can only be estimated, and will lead to a systematically reduced polarization. To compensate for the transverse fringing fields two sets of magnetic deflection coils replaced the electrostatic deflection plates previously used. The conservation of $\vec{S}\cdot\vec{p}$ in a magnetic field means that the spin rotation induced when the beam is deflected by the polarimeter fringing fields will be canceled by the compensating deflection of the magnetic coils. The success of this improvement is shown in the SR curve (Fig. 6)

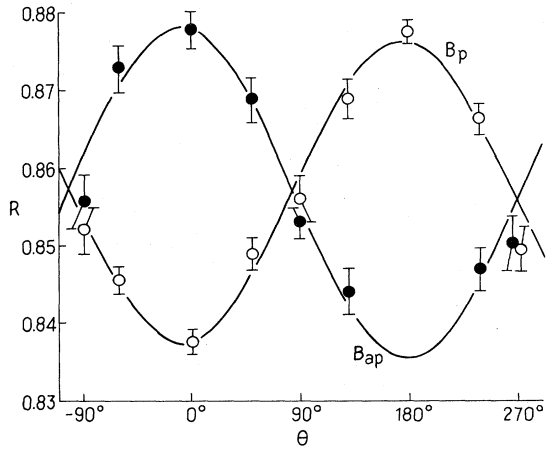

FIG. 6. Ratio of perturbed to unperturbed o-Ps events (R) is plotted vs the angle θ between $\vec{S}$ and $\vec{B}$. Defining θ with respect to B_p, the magnetic field parallel to the beam velocity, distinguishes the data acquired in the antiparallel field B_{ap} from the data acquired in B_p. The data were fit to the equation $\bar{R}=R[1\pm c\cos(\theta+\phi)]$ where the $-$ $(+)$ sign was used for B_p (B_{ap}), $\bar{R}$ is the ratio that would be obtained for an unpolarized beam $c=f\eta P$, θ is the Wien filter rotation angle, and ϕ is a phase shift in $\vec{P}$ due to polarimeter fringing fields. The X^2 per degree of freedom of the least-squares fit were 5.3/4 for B_p and 6.4/5 for B_{ap}.

where the phase shift ϕ is less than 5°. Thus, any reduction in P due to spin rotation by stray transverse fields is $\Delta P/P < 0.004$. Combining the errors of the three systematic effects discussed above, we estimate the instrumental error in the measured polarization of the slow-positron beam to be $\Delta P/P = 0.04$.

III. RESULTS

In this section we will present our major findings. We show it is possible to achieve a highly polarized ($P = 0.69 \pm 0.04$) slow-positron beam by selectively absorbing source positrons which are emitted at low energies and large angles relative to the normal. We also show the evidence that the beam polarization is independent of moderator atomic number (Z), but does depend on the Z of the absorber. In addition, we have confirmed the high source-to-slow-positron conversion efficiency reported[14] for metallic-strip moderators. We have measured the efficiency and energy spread of five moderators as well as the effect of both low-Z and high-Z absorbers on the slow-positron yield.

A. Polarization results

As shown in Fig. 7, the polarization of the slow-positron beam increases dramatically as absorbers of increasing thickness but low atomic number are placed between the source and moderator. This effect can be understood qualitatively by noting that the absorber will preferentially pass positrons which were emitted from the source at high energy (and hence with large helicity). In addition, positrons emitted at large angles with respect to the normal to the source (which have a reduced polarization component along the beam direction) must penetrate larger absorber thicknesses and are thus preferentially removed from the beam. This angular selection effect is also seen in Fig. 7 in the difference between results using the 2π-sr source and those of the π-sr source. A quantitative discussion of the results will be presented in Sec. IV. The lack of dependence of beam polarization on moderator atomic number shown in Fig. 7 is displayed in Table I. For these measurements the same source (2π sr), absorber (46 mg/cm^2 Be), and source-absorber-moderator geometry were used. The polarizations for four moderators are equal within one standard deviation and the fifth agrees within two. The implications of this result on the slow-positron emission process will be discussed in Sec. IV. The lack of additional depolarization of the positrons in the high-Z moderators is contrasted with the effect of high-Z absorbers on slow-positron polarization shown in Fig. 8. Again, a quantitative discussion will be presented later.

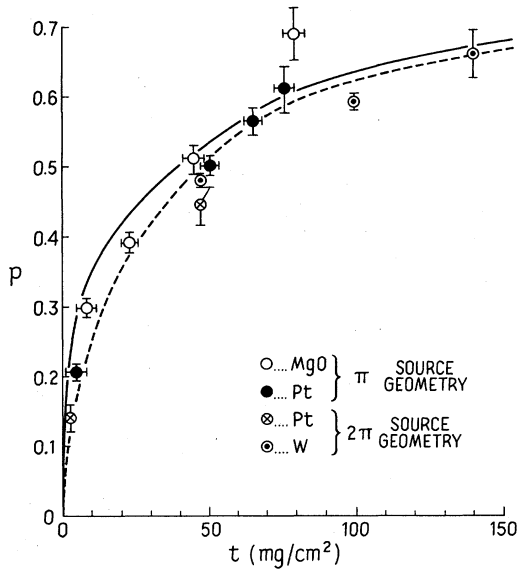

FIG. 7. Slow-e^+ polarization measured for different thicknesses t of beryllium ($Z=4$) or plastic ($\bar{Z}=6$) absorbers placed between the source and moderator. The solid curve is calculated from Eq. (6) for the π-sr ^{22}Na source and the dashed curve is calculated for the 2π-sr ^{22}Na source. The polarizations shown were measured using the MgO, Pt, and W moderators. The uncertainties shown are based on Poisson ($\sqrt{N}$) statistics.

In addition, under the same conditions discussed above, we made a preliminary measurement of the polarization of positrons from a ferromagnetic (silicon-steel) moderator. The measured polarizations were $P = 0.33 \pm 0.04$ for a magnetized sample, and $P = 0.29 \pm 0.04$ for an unmagnetized sample. This shows that the interaction of the slow e^+ with unpaired electron spins in the moderator can give rise to substantial depolarization.

TABLE I. Measured polarization P, slow-emission efficiency ϵ, and energy spread (full width at half-maximum intensity) ΔE, for five moderators. All measurements were made with the same source and source-moderator geometry, as discussed above.

Material	Z	P	ϵ	ΔE (ev)
Pt	78	0.442±0.025	$(2.0\pm0.5)\times10^{-4}$	1.2
W	74	0.480±0.008	$(1.3\pm0.4)\times10^{-3}$	2.1
Ta	73	0.463±0.019	$(4\ \pm1)\times10^{-5}$	0.7
Mo	43	0.460±0.015	$(6.0\pm1.5)\times10^{-4}$	1.7
MgO	10.4	0.472±0.015	$(1.0\pm0.3)\times10^{-4}$	5

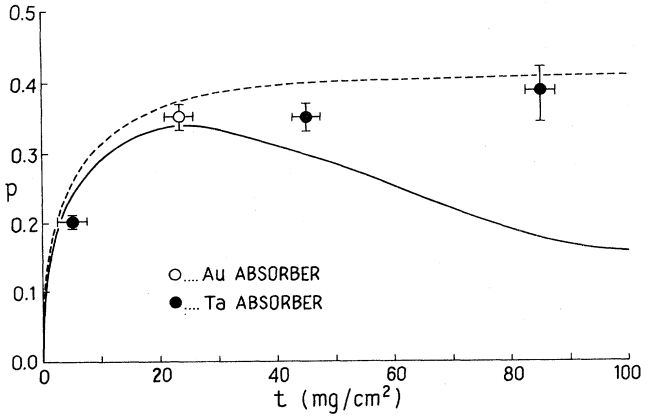

FIG. 8. Polarization of the slow e^+ emitted from the Pt moderator after transmission through gold ($Z=79$) or tantalum ($Z=73$) absorbers of different thickness placed between the source and moderator. Comparison with Fig. 7 shows the substantial depolarization which occurs in high-Z absorbers. The solid curve is calculated from Eq. (6) using the depolarization $D(E)$ calculated in Ref. 6 for positrons stopping in semi-infinite media with $Z=73$. The dashed curve uses our estimate of the depolarization in *transmission* through $Z=73$ absorbers, as discussed in the text.

B. Positron emission efficiency and energy-spread measurements

As first reported by Dale, *et al.*,[14] metallic-strip moderators are highly efficient when well annealed. Our results for W, Pt, Ta, and Mo moderators are shown in Table I. The efficiency is defined as the slow-positron beam flux, corrected for the measured 60% beam transmission (between the entrance of the CMA and the entrance to the polarimeter), divided by total source-positron flux, using the New England Nuclear Corp.-assayed activity. Moderator preparation is described in the Appendix.

The energy width was measured with a three-grid retarding field analyzer placed immediately following the moderator. It should be noted that the energy spread of the slow-positron spectrum causes the measured moderator efficiency to depend on positron-beam optics. For example, in a second electrostatically focused beam used at Michigan, the W moderator was found to be only twice as efficient as the Pt,[15] and in a beam using optics which accept only a very narrow energy width and angular dispersion, the efficiencies of the two moderators were identical.[16]

Absorbers reduce the flux of positrons from a radioactive source exponentially with increasing thickness.[17–19] The e-folding thickness (t_0) depends on source end-point energy, but only weakly ($Z^{-1/3}$) on the atomic number of the absorber. For a ^{22}Na source and Al absorbers, $t_0=24.3$ mg/cm^2.[18] Our measurements of the slow-positron flux as a function of absorber thickness, made with absorbers from 15 to 140 mg/cm^2 thickness, give $t_0=26.2\pm0.4$ mg/cm^2 for Be ($Z=4$), $t_0=25.5\pm0.4$ mg/cm^2 for plastic scintillator ($\bar{Z}=6$), and $t_0=23.5\pm0.2$ mg/cm^2 for Ta ($Z=73$). These are in agreement with the results for the entire positron spectrum obtained in Ref. 18 and with the results of Ref. 19 for slow positrons.

The positron conversion efficiency also depends on source design. The smaller solid angle afforded by the conically shaped depression of the 22 mCi π-sr source reduces by a factor of 2 the fraction of positrons incident on the moderator. In addition, the thicker deposit of source material (6 ± 2 mg/cm^2 versus only 1 mg/cm^2 in the other source) absorbs an additional 12%, leaving this source 44% as efficient in producing slow positrons as the 2π-sr source.

IV. DISCUSSION

In this section we will develop a theoretical model for the polarization of the slow-positron beam and compare it with the measurements presented in Sec. III. From this comparison we can draw conclusions about the portion of the source-positron energy spectrum selected by the moderator in its formation of slow positrons.

The projection on the beam axis ($\hat{N}$) of the spin $\vec{\sigma}_i$ of the ith positron emitted by a nucleus at an angle θ_i and kinetic energy E_i is $\vec{\sigma}_i\cdot\hat{N}=\beta(E_i)\cos\theta_i$. The quantity $\beta(E_i)=\{1-[m_0c^2/(E_i+m_0c^2)]^2\}^{1/2}$ where m_0c^2 is the positron rest energy. If there were no changes in spin direction, the beam polarization would just be an average over the energy and angle of source positrons which contribute to the slow-positron beam, that is, $P=\langle\vec{\sigma}_i\cdot\hat{N}\rangle$. However, the source holder, absorbers, and moderator can modify the spin direction. The source holder will backscatter[20] an angle-averaged fraction $b(E)$ of spin-reversed positrons into the forward direction. We ignore depolarization of the small number of backscattered positrons, but include depolarization in the absorber and moderator where collisions result in depolarization in the amount $1-D(E_i,Z)$, where E_i is the kinetic energy on entrance into the material and Z the respective atomic number (we use "a" to indicate absorber, "m" to indicate moderator). The final spin projection is then

$$\vec{\sigma}_i\cdot\hat{N}=\beta(E_i)\cos\theta_i[1-b(E_i)]D(E_i,Z_a)D(E_i-E_l,Z_m)\ , \tag{4}$$

where we have allowed an energy loss E_l in the absorber.

The appropriate energy and angle ensemble average must now be found. The distribution of source positrons as a function of energy is $N(E)$, increased to $N(E)[1+b(E)]$ by backscattering in the source holder. (The subscripts on E and θ have been dropped for convenience in these and all subsequent expressions.) Absorption in the source, the source-holder window, and added absorbers reduce the intensity according to the formula e^{-z/t_0}, where $z=t\sec\theta$ is the path length through the absorber of thickness t, and t_0 is the e-folding length measured as described above. In the absorber the positrons lose an amount of energy $E_l(z)$, removing positrons with source energy less than $E_l(z)$ from the spectrum.[17] The energy spectrum of the remaining positrons may be approximated by a spectrum identical in shape to the source spectrum.[17] The yield of slow positrons per source posi-

tron striking the moderator is defined to be $y(E-E_l)$. One of the results of this work is to put limits on the high-energy shape of the yield function y.

The acceptance of positrons emitted at angle θ to the normal is limited primarily by the source holder. For the π-sr source the maximum angle $\theta_m=\pi/3$, while for the 2π-sr source $\theta_m=\pi/2$. Scattering in the source, the Ti window, and, primarily, in the absorber, effectively randomizes positron directions so that additional angular selectivity obtained by letting the moderator accept only a narrow forward-directed cone of positrons was found to have no measurable effect on the polarization.

From the above discussion, we may write a general expression for the polarization P

$$P=\frac{\int_0^{\theta_m}\cos\theta\sin\theta\,d\theta\int_{E_l}^{E_m}dE\,N(E)y(E-E_l)\beta(E)B(E)D(E,Z_a)D(E-E_l,Z_m)e^{-t\sec\theta/t_0}}{\int_0^{\theta_m}\sin\theta\,d\theta\int_{E_l}^{E_m}dE\,N(E)y(E-E_l)e^{-t\sec\theta/t_0}}, \tag{5}$$

where $B(E)=[1-b(E)]/[1+b(E)]$. We note that the lack of depolarization in high-Z moderators, in contrast to the depolarization evident in high-Z absorbers which is small only at low kinetic energies, suggests that only positrons with $E-E_l\approx 0$ are effective in forming slow positrons. [This conclusion is qualitatively consistent with determinations of $y(E)$ by Mills.[21]] For a first approximation, then, we let $y(E-E_l)=\delta(E-E_l)$, where δ is the Dirac δ function. Using the fact that $D(0,Z)=1$, we obtain

$$P=\beta(E_l)B(E_l)D(E_l,Z_a)\frac{\int_0^{\theta_m}\cos\theta e^{-t\sec\theta/t_0}\sin\theta\,d\theta}{\int_0^{\theta_m}e^{-t\sec\theta/t_0}\sin\theta\,d\theta}. \tag{6}$$

Numerical integrations of Eq. (6) give the curves shown in Fig. 7 and the solid curve in Fig. 8. The experimental data agree with the calculated curves in Fig. 7 to within 10%, justifying the approximation $y(E-E_l)=\delta(E-E_l)$. The 2π-sr source displays on average $\sim 10\%$ lower polarization than the π-sr source, but its higher efficiency more than compensates for the lower P, as will be discussed.

The experimental data shown in Fig. 8 are substantially above the curve calculated using the theory of Ref. 6 for the depolarization $D(E,Z)$ of positrons stopping in a semi-infinite medium. This theory is not strictly valid for positrons transmitted through an absorber, however, since positrons suffering large angle scattering and correspondingly larger depolarization are not transmitted. Indeed, it can be crudely estimated that the depolarization of positrons in transmission $[D_T(E,Z)]$ will be reduced from that calculated in Ref. 6 to $D_T(E,Z)=D(E,Z)\times\{[1-b(Z)]/[1+b(Z)]\}$, where $b(Z)$ is the backscattering coefficient.[20] The dashed curve in Fig. 8, which includes this correction, is in better agreement with the experiment data. In light of our results, we believe a rigorous calculation of $D_T(E,Z)$ is now of interest.

Because of the good agreement between the experimental data and $D_T(E,Z)$, we can, with considerable confidence, use the calculations of $D(E,Z)$ in Ref. 6 to find the characteristic kinetic energy of those source positrons stopping in the moderator which are effective in forming slow positrons. Bouchiat and Lévy-Leblond (Ref. 6) show that the ratio of final polarization P_f to initial polarization P_I is given by

$$\frac{P_f}{P_I}=\exp\left[-C\frac{\langle Z(Z+1)\rangle}{\langle Z\rangle}\int_{E_f}^{E_I}R\,dE\right]$$
$$\approx\exp\left[-C\frac{\langle Z(Z+1)\rangle}{\langle Z\rangle}\sum_{E_f}^{E_I}R\Delta E\right], \tag{7}$$

where R and C are discussed in Ref. 6, and E_I and E_f are the energies of the positron before and after passage through the depolarizing medium. Equation (7) shows that the depolarization suffered by positrons in matter depends on both Z and the amount of energy lost. Figure 9 shows the measured variation of the slow-e^+ polarization as a function of Z. A least-squares fit of Eq. (7) to these data results in a slope $-C\sum_{E_f}^{E_I}R\Delta E=(0\pm 2)\times 10^{-4}$. The factors R and C can be found from Figs. 1 and 2 of Ref. 6, and E_f is taken as thermal energy. We interpret

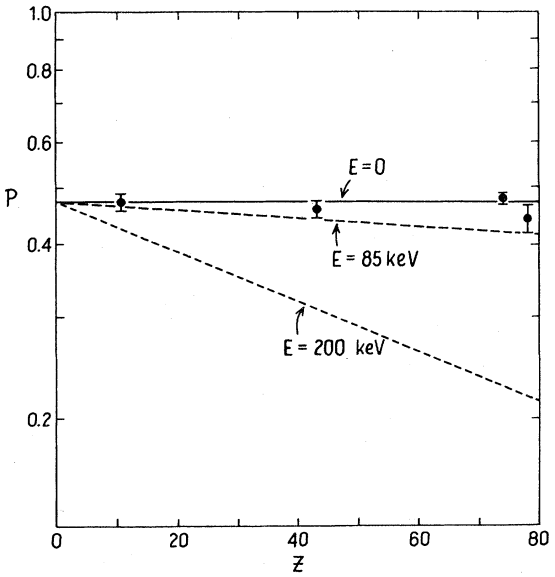

FIG. 9. Variation of slow-e^+ polarization with moderator atomic number Z. As discussed in the text, fitting these data to Eq. (7) allows us to conclude that the characteristic energy of positrons entering the moderator which emerge as slow positrons is less than 17 keV.

the limit on E_I found by this procedure, $E_I < 17$ keV, to be the characteristic or approximately average energy of source positrons entering the moderator which result in slow positrons, i.e., $E_I \equiv \bar{E}$. We note that we have assumed that $\bar{E}$ is independent of the moderator material, an assumption we will justify shortly.

We now calculate the average energy of positrons which are moderated using the efficiency of slow-positron production for monoenergetic positrons of energy 300 eV $\leq E \leq 3$ keV measured by Mills.[21] Mills fits his data to the equation $y(E)=y_0[1+(E/E_0)^n]^{-1}$, where y_0, E_0, and n are constants which depend on the specific moderator material. The zero energy yield y_0 is between 0.1 and 0.5 for atomically clean metals, $n \sim 1.6$, and E_0 is typically between 3 and 25 keV. We can combine this yield function with the ^{22}Na spectrum $N(E)$ to calculate the predicted mean kinetic energy

$$\bar{E}_C = \frac{\int_{E_l}^{E_m} N(E) y(E-E_l) E\, dE}{\int_{E_l}^{E_m} N(E) y(E-E_l) dE} . \tag{8}$$

Using values of n, y_0 and E_0 from Ref. 21, we find that $\bar{E}_C \simeq 85$ keV, and that due to the shape of the β spectrum, $\bar{E}_C$ decreases slowly with increasing n and is essentially independent of E_0, justifying the assumption made above of equal $\bar{E}$ for each moderator. The value of $\bar{E}_C$ is only weakly dependent on the details of the high-energy end of the β spectrum. The predicted value of $\bar{E}_C \simeq 85$ keV would result in $P=0.40$ for the W moderator, in 8σ disagreement with the experimental polarization. It should be noted that Eq. (8) takes the source positrons to be incident on the moderator in a direction perpendicular to the plane of the moderator surface. However, all possible source-absorber combinations result in an isotropic angular distribution of source positrons. This will reduce the average kinetic energy perpendicular to the moderator surface resulting in shallower implantation depths, thus, allowing positrons with higher than predicted initial kinetic energies to diffuse to the surface and form slow positrons. Thus the value $\bar{E}_C = 85$ keV calculated from Eq. (8), using $y(E)$ of Ref. 21, must be considered a lower limit, rendering the disagreement between theory and experiment even more severe than stated above. This disagreement shows that the yield function $y(E)$ measured for $E \leq 3$ keV, cannot be simply extrapolated to high energies.

The derivation of $y(E)$ assumes an exponential positron implantation profile with mean depth proportional to E^n followed by diffusion of the thermalized e^+. Recently, unpublished Monte Carlo simulations[22] of positron implantation in metals conclude that the implantation profile is not exponential and suggests that the yield function that would result would be smaller at higher energies than $y(E)$, which would decrease $\bar{E}_C$, bringing it into better agreement with our experimental work.

The good agreement between the calculated and measured polarization in Fig. 5 places strong limits on the possibility that field ionization of o-Ps at the moderator surface plays a significant role in slow-positron formation in MgO.[7] The formation of Ps results in a spin mixing in the $m=0$ states of Ps on a time scale characteristic of the hyperfine frequency ν_{HF}. If the Ps formed within the grain lives as long as $\tau = 1/\nu_{\mathrm{HF}} = 5\times 10^{-12}$ sec before being ionized, the positron would suffer a 50% depolarization. The fraction of slow positrons (f_s) which is formed in this way can thus be shown to be less than 20% from the relation

$$f_s \leq \frac{1}{0.5}\frac{P_c - P_e}{P_c} , \tag{9}$$

where P_c is the calculated polarization and P_e the measured polarization. Similar reasoning suggests that depolarization in the process of diffusion and emission of slow positrons in nonferromagnetic moderators is also very small. On the other hand, the 33% depolarization of slow positrons from ferromagnetic moderators relative to the nonferromagnetic moderators of Table I shows that substantial depolarization can take place during the diffusion and emission processes.

V. APPLICATIONS

The results displayed in Fig. 7 show that intense beams of slow e^+ with polarizations ranging from $P=0.13 \pm 0.01$ to 0.66 ± 0.03 may be generated using the high efficiency W moderator. The choice of P to be used in a particular experiment depends upon the experimental conditions. In experiments which search for small polarization dependent asymmetries, it is traditional to optimize the quantity $P^2 I$.[23] Using the results of Fig. 7 and the measured absorber attenuation shows that the maximum value of $P^2 I$ occurs for a 40 mg/cm^2 Be absorber, where $\epsilon = 3\times 10^{-4}$ and $P=0.45$. On the other hand, when experiments are limited by systematics rather than statistics, the maximum possible value of P should be chosen, consistent with a reasonable running time. Calculations made using Eq. (6) show that the polarization peaks at ~ 150 mg/cm^2 absorber thickness with a value $P=0.72$, slowly falling with thicker absorbers due to increasing depolarization. The polarization and yield depend on source end-point energy. Could another positron source be better than ^{22}Na? Additional calculations indicate that the highest intensity slow-e^+ beam for 150 mg/cm^2 absorber occurs for a source with an end-point energy $E_m \simeq 1$ MeV, suggesting that ^{11}C, provided on line using a Van de Graaff accelerator, could provide the highest polarization of all sources.

The development of a high-polarization, high-intensity, slow-positron beam has already played a crucial role in the demonstration of a new quantitative probe of the surface magnetic properties of ferromagnetic materials.[3] The use of polarized slow positrons to form positronium on ferromagnetic metals satisfies the experimental requirements of spin sensitivity and surface selectivity since (1) the spin states of Ps are sensitive to the relative orientation of the spin polarization $\vec{P}_{e^-}$ of the surface electrons and $\vec{P}_{e^+}$, the polarization of the positron beam; (2) electron capture to form Ps can only occur at the surface of a metal due to the screening of the positron in the bulk by the valence electrons.

In order to determine $\vec{P}_{e^-}$, an asymmetry in the forma-

tion of triplet Ps is measured upon reversal of either $\vec{P}_{e-}$ or $\vec{P}_{e+}$, with triplet Ps distinguishable by its long (142 nsec) lifetime. This asymmetry is given by

$$A = \tfrac{1}{3}\vec{P}_{e+}\cdot\vec{P}_{e-} . \quad (10)$$

Measurement of A and $\vec{P}_{e+}$ thus allows the determination of $\vec{P}_{e-}$. Preliminary measurements[3] have demonstrated the feasibility of this new surface probe.

The technique of measuring changes in the relative intensity of the spin states of Ps can also be exploited to measure other electron spin-polarization effects. For instance Ps could be formed in a pellet of a paramagnetic salt, such as Gd_2O_3 placed in a high magnetic field and cooled to low temperatures. Measurement of the asymmetry in o-Ps formation upon reversal of $\vec{P}_{e+}$ would provide information on the relative electron capture cross sections between paramagnetic and nonparamagnetic ions. We note that the factor of $\frac{1}{3}$ in Eq. (10) is replaced by unity when Ps is formed in a high magnetic field, allowing values of A as high as 100%.

A somewhat more unusual application of this technique tests the proposed[24] causal link between parity violation in nuclear β decay and the seemingly parity-violating optical activity characteristic of the biomolecules on which terrestrial life is based. The largest causal mechanism predicted to occur[25] is a difference of order 10^{-10} in the electron ionization rates for L vs D isomers of amino acids when bombarded by 100-keV β-decay electrons. The mechanism also results in an asymmetry of order $A_{Ps}\approx 10^{-5}$ in the relative intensities of the singlet and triplet states of positronium upon interchange of L and D isomers of an optically active target or upon helicity reversal of the slow-e^+ beam.

Recently, a slow-positron beam with an initial helicity $h_0 = 0.21\pm 0.02$ was used to measure or set limits on the size of A_{Ps}. No asymmetry was observed at the 7×10^{-4} level in two amino acids. With an increase in the beam polarization (and thus h_0) to $P=0.5$ by the methods outlined in this paper and further improvements in the experimental technique over Ref. 2, we have found no asymmetry in leucine at the level of 1.0×10^{-4}.[26]

The 33% depolarization suffered by the slow e^+ emitted by the silicon-steel moderator shows that polarized slow positrons can be used to study the interactions of positrons in ferromagnetic materials. A monoenergetic slow-e^+ beam of known polarization could be remoderated[26] in a well-characterized ferromagnetic single-crystal moderator, and the change in polarization of the remoderated e^+ measured. Varying the energy of the positrons incident on the remoderator will vary the number of interactions the positron undergoes prior to thermalization, which may cause a change in the measured final polarization. At low incident energies predominantly the surface layers will be sampled, providing an independent measurement of surface magnetization. Finally, coating the remoderator surface with paramagnetic molecules[27] or ferromagnetic monolayers may change the polarization of the remoderated positrons.

Scattering of polarized slow e^+ from surfaces or through gases can yield information which supplements electron scattering experiments. An example of this would be the substitution of polarized low-energy positron diffraction (PLEPD) for polarized low-energy electron diffraction (PLEED) as a consistency check on crystal-structure models, with a major difference being that exchange plays no role in PLEPD. The experimental and theoretical aspects of PLEPD are further discussed in Refs. 1 and 13.

Finally, the physics of slow-positron formation results in the novel feature that the combination of absorber and moderator acts as a low-resolution energy spectrometer, with a 40 mg/cm^2 Be absorber, for example, selecting slow e^+ from source positrons with initial energies of 100 ± 35 keV.

ACKNOWLEDGEMENTS

We would like to thank D. W. Gidley, A. Rich, M. Skalsey, and T. Girard for useful discussions, K. Kikuchi for major equipment loans, H. Carter, formerly of New England Nuclear Corp., for willing assistance in source design and preparation, and K. Coulter and T. Moylan for contributions to the construction phase of this experiment. This work is supported by the National Aeronautics and Space Administration (Grant No. NSG7452), by the National Science Foundation (Grants Nos. PHY81-07573 and PHY81-09269), the Office of the Vice President for Research of the University of Michigan, and the University of Michigan—Dearborn Campus Grants Committee.

APPENDIX: DETAILS OF METALLIC MODERATION PREPARATION

An efficient moderator using untreated, commercial-grade metal was developed which uses dental-grade, well-annealed Pt foil 0.02 mm thick (Degussa GB Dental and Goldhalbzeug, Frankfurt, West Germany). Parallel slits, 2 cm long, 1 mm apart, were carefully cut in a 3×3 cm foil. The resulting strips were bent 45° or 90° to form a Venetian blind. The slow-positron yield, two times higher than the MgO smoked "Hexcell" moderator, was found to be reduced by a factor of 5 when MgO was smoked on the Pt vanes. Excessive flexing with the resultant work hardening of the vanes also decreased the yield, demonstrating that the lack of bulk defects is responsible for the high yield of slow positrons. We note that previous tests of annealed Pt have given inconsistent results.[14,28]

Tungsten-strip moderators, prepared in a manner similar to those described by Dale *et al.*[14] and Canter[29] were also tested. A 20-cm long, 1.2-mm wide strip was cut off a 0.025-mm thick sheet and heated to over 2200 °C by passing current through it in a vacuum better than 5×10^{-8} Torr. The strip was then cut into 12 mm lengths and clamped at the ends to form a moderator consisting of seven parallel vanes separated by 1.5 mm. The strips were cleaned with acetone before heating, but the etching treatment described in Ref. 20 was found to have no effect on yield or polarization. Similarly the cooling rate (slow, $\sim 100°$ drop per minute; or fast, current turned off or strip broken) has no measurable effect. However, the temperature and length of time of heating were important. Eleven

strips were heated for 5 min at 2200 °C. A few strips which were heated to 2400 or 2700 °C for 5 min showed 20—50 % larger yields. One strip heated to 2200 °C for 12 h showed a yield comparable to those heated to 2700 °C. This heating allows crystals to grow,[30] reducing the number of grain boundaries at which positrons may be trapped.

Similar moderators were made of Ta, Mo, and Cu, heated to temperatures as high as 90% of the melting point. The first two metals are excellent moderators, but Cu, while initially showing a good yield, degraded seriously in a few hours. While a slow loss of yield was also observed for the Ta moderator, exposure of a W moderator to air for four weeks produced less than 30% loss of slow positrons. Use of a W moderator in the beam for six months resulted in a 50% drop in beam strength, probably due to radiation-induced defects.

[1]P. W. Zitzewitz, J. Van House, A. Rich, and D. W. Gidley, Phys. Rev. Lett. 43, 1281 (1979).
[2]D. W. Gidley, A. Rich, J. Van House, and P. W. Zitzewitz, Nature (London) 297, 639 (1982).
[3]D. W. Gidley, A. Köyman, and T. W. Capehart, Phys. Rev. Lett. 49, 1779 (1982).
[4]I. J. Rosenberg, A. H. Weiss, and K. F. Canter, Phys. Rev. Lett. 44, 1139 (1980).
[5]A. P. Mills, Jr., in *Proceedings of the International School of Physics, "Enrico Fermi", Course LXXXIII, Varenna, 1981,* edited by W. Brandt and A. Dupasquier (Academic, New York, 1982) and references therein.
[6]C. Bouchiat and J. M. Lévy-Leblond, Nuovo Cimento 33, 193 (1964).
[7]T. C. Griffith, G. R. Heyland, K. S. Lines, and T. R. Twomey, Phys. Lett. 69A, 169 (1978).
[8]L. M. Langer, Rev. Sci. Instrum. 20, 216 (1949).
[9]P. W. Zitzewitz, J. Appl. Phys. 51, 856 (1980).
[10]A. P. Mills, Jr., Appl. Phys. 23, 1715 (1980).
[11]D. W. Gidley, Ph.D. thesis, University of Michigan, 1980 (unpublished) (available from University Microfilms, Ann Arbor, Michigan).
[12]G. Gerber, D. Newman, A. Rich, and E. Sweetman, Phys. Rev. D 15, 1189 (1977).
[13]A. Rich, Rev. Mod. Phys. 53, 127 (1981).
[14]J. M. Dale, L. D. Hulett, and S. Pendyala, Surf. Int. Anal. 2, 199 (1980).
[15]D. W. Gidley (private communication).
[16]A. Deuring, K. Floeder, D. Fromme, W. Raith, A. Schwab, G. Sinapius, P. W. Zitzewitz, and J. Krug, J. Phys. B 16, 1633 (1983).
[17]R. Evans, *The Atomic Nucleus* (McGraw-Hill, New York, 1955), p. 611.
[18]L. E. Spanel, A. S. Rupaal, and J. R. Patrick, Phys. Rev. B 8, 4072 (1973).
[19]L. D. Hulett, J. M. Dale, and S. Pendyala, Surf. Int. Anal. 2, 204 (1980).
[20]H. H. Seliger, Phys. Rev. 88, 408 (1952).
[21]A. P. Mills, Jr., Phys. Rev. Lett. 41, 1828 (1978).
[22]R. M. Nieminen (private communication).
[23]J. Kessler, *Polarized Electrons* (Springer, New York, 1976).
[24]F. Vester, T. L. Ulbricht, and H. Krauss, Naturwisschaften 46, 68 (1959).
[25]R. A. Hegstrom, Nature 297, 643 (1982).
[26]J. Van House, A. Rich, and P. W. Zitzewitz, Origins of Life (Reidel, Holland, in press).
[27]D. A. Fisher, K. G. Lynn, and W. E. Frieze, Phys. Rev. Lett. 50, 1149 (1983).
[28]K. G. Lynn and B. T. A. McKee, Appl. Phys. 19, 247 (1979).
[29]K. F. Canter and A. P. Mills, Jr., Can. J. Phys. 60, 551 (1982).
[30]C. S. Robinson, Jr., J. Appl. Phys. 13, 647 (1942).